IVYSPRING INTERNATIONAL PUBLISHER

Theranostics

2019; 9(1): 48-64. doi: 10.7150/thno.29715

Research Paper

CD44 Assists the Topical Anti-Psoriatic Efficacy of Curcumin-Loaded Hyaluronan-Modified Ethosomes: A New Strategy for Clustering Drug in Inflammatory Skin

Yongtai Zhang*, Qing Xia*, Yanyan Li*, Zehui He*, Zhe Li, Teng Guo, Zhonghua Wu, Nianping Feng✉

Department of Pharmaceutical Sciences, Shanghai University of Traditional Chinese Medicine, Shanghai 201203, China

*Authors contributed equally to this work

✉ Corresponding author: E-mail addresses: npfeng@hotmail.com; npfeng@shutcm.edu.cn

Received: 2018.09.04; Accepted: 2018.11.13; Published: 2019.01.01

Abstract

Background: Psoriasis is a common chronic inflammatory skin disease. Its treatment is challenged by the limited amount of drug reaching the inflamed skin. The overexpressed CD44 protein in inflamed psoriatic skin can serve as a potential target of novel active-targeting nanocarriers to increase drug accumulation in the skin.

Methods: Hyaluronic acid (HA) was linked to propylene glycol-based ethosomes by covalent binding to develop a novel topical drug delivery carrier (HA-ES) for curcumin. An imiquimod-induced psoriasis mouse model was established, and curcumin delivery and anti-psoriatic efficacy using HA-ES were compared with those using plain ethosomes (ES).

Results: The HA gel network formed on the surface of HA-ES reduced the leakage and release of poorly water-soluble curcumin. Compared with ES, transdermal curcumin delivery was significantly enhanced by using HA-ES as vehicles; the cumulative transdermal amount and the amount retained in the skin *in vitro* after 8 h were, respectively, 1.6 and 1.4 times those observed with ES, as well as 3.1 and 3.3 times those observed with a curcumin propylene glycol solution (PGS), respectively. The *in vivo* psoriatic skin retention of curcumin with HA-ES was 2.3 and 4.0 times that of ES and PGS, respectively. CD44 expression in imiquimod-induced psoriasis-like inflamed skin was 2.7 times that in normal skin. Immunostaining revealed similar results, suggesting that the specific adhesion of HA-ES to CD44 increased drug accumulation in the skin. After topical administration to mice, the HA-ES group showed an alleviation of inflammation symptoms; lower TNF-α, IL-17A, IL-17F, IL-22, and IL-1β mRNA levels; and lower CCR6 protein expression compared to the ES and PGS groups.

Conclusion: We demonstrated increased topical drug delivery of curcumin to inflamed tissues using HA-ES targeting the highly expressed CD44 protein. This innovative strategy could be applied for the development of topical drug delivery systems targeting inflamed skin.

Key words: nanomedicine, liposomes, transdermal, bioadhesive, targeting

Introduction

Psoriasis is a chronic, inflammatory, immune-mediated hereditary disease that is prone to recurrence and causes systemic damage. The major histopathological changes are neovascularization, hyperplasia of keratinocytes, and inflammatory cell infiltration [1]. Topical administration is one of the important approaches to treat psoriasis. The drug is applied directly to the affected skin and can directly work on the inflammatory region to improve the symptoms of psoriasis. For some drugs with a narrow therapeutic window, topical administration can reduce the systemic absorption compared to oral and

injection routes, thereby reducing adverse systemic effects. In addition, topically applied drugs are released slowly into the skin, thereby providing a prolonged duration of action, reducing the frequency of administration, and increasing patient compliance. However, the stratum corneum (SC) limits the amount of drug being percutaneously absorbed, resulting in drug wastage and poor clinical efficacy after topical administration. To prevent the poor accumulation of drugs in the inflamed skin, the formulation of drugs using nanocarriers such as microemulsion, lipid nanoparticles, and liposomes has gained importance [2]. Liposomes are completely enclosed small vesicles with a phospholipid bilayer. Fat-soluble drugs can be dispersed in its lipid bilayer, and water-soluble drugs can be contained in its aqueous core. Liposomes possess excellent biocompatibility and can entrap various types of drugs. Classic liposomes mainly improve the hydration of the SC. By fusing with the SC, liposomes change the structure of the SC and disrupt its lipid arrangement, which allows the encapsulated drug molecules to permeate the intercellular spaces via diffusion and capillary action, thereby enhancing the percutaneous absorption of drugs [3]. However, owing to the rigid membrane of the classic liposome, its permeation across deep skin layers through SC fissures is limited. By adding edge activators such as cholic acid, Tweens, and Spans, the phospholipid membrane is softened and its deformability is increased [4]. However, the addition of a surfactant may reduce the biocompatibility of the liposome. Ethosomes, first reported by Touitou, are novel deformable liposomes prepared by dispersing liposomes in 20–45% solutions of small-chain biocompatible alcohols such as ethanol, propylene glycol, and glycerol [5]. This increases the fluidity of the phospholipid membrane. Besides, the small-chain alcohols contained in the liposomal system can greatly increase the loading of fat-soluble drugs [6]. The percutaneous permeability of the ethosomes is demonstrated to be superior to that of classic liposomes, and the skin retention of the drug is also significantly increased [7]. However, plain nanocarriers for topical delivery, including ethosomes, do not specifically target the site of skin disease and simply cause drug accumulation and diffusion during topical absorption. In addition, the stability of liposomal vesicles also limits the commercial production of ethosomes.

Recent studies have found that in the epidermis of psoriatic inflamed skin, the CD44 protein is highly expressed and hyaluronic acid (HA) distribution is markedly reduced, suggesting that overexpressed CD44 protein can serve as a potential target of novel active-targeting nanocarriers for topical administration to increase skin drug retention and enhance drug efficacy [8]. HA, a natural ligand for the CD44 protein is widely used in targeted nano-drug delivery systems to improve the targeting efficiency and increase the drug concentration in the lesion site, thus enhancing the therapeutic effect whilst reducing toxic adverse effects [9].

In the present study, we constructed HA-modified ethosomes (HA-ES; Fig. 1A) as a novel nano-topical drug delivery system targeting CD44 in the inflamed epidermis as a vehicle for curcumin, a poorly water-soluble drug. An imiquimod-induced psoriasis mouse model was established, and curcumin delivery and anti-psoriatic efficacy using plain ethosomes (ES) were compared with those using HA-ES. The feasibility of the topical administration of HA-modified nanocarriers to target inflammatory skin diseases involving high CD44 expression was analyzed.

Materials and Methods

Materials

DSPE-PEG2000 and hydrogenated soybean phospholipids (HSPC) were obtained from Nippon Fine Chemical Co., Ltd. (Japan); dioleoyl phosphoethanolamine (DOPE) was purchased from Lipoid GmbH (Germany); HA (MW = 240 kDa) was obtained from Freda Biochem Co., Ltd. (China); and curcumin was purchased from Chengdu Mansite Bio-Technology Co., Ltd. (China). Imiquimod cream (5%, w/w) and clobetasol propionate cream (0.02%, w/w) were from Mingxin Pharmaceutical Company (China) and Shanghai General Pharmaceutical Co., Ltd. (China), respectively. Tris-buffered saline with Tween 20 (TBST) was from Shanghai Yeasen Biotechnology Co., Ltd. (China). Ponceau S, BCA working solution, and SDS-PAGE loading buffer were obtained from Beyotime® Biotechnology (China). ECL luminescence reagent was from Sangon Biotech (Shanghai, China). Diethyl pyrocarbonate (DEPC) was purchased from Sigma-Aldrich LLC (USA). Recombinant human TNF-alpha protein (TNF-α) was supplied by R&D Systems (USA). 3,3-Diaminobenzidine tertrahydrochloride (DAB) developer was from Sangon Biotech. Trizol® reagent (Trizol) was purchased from Invitrogen™ (Thermo Fisher Scientific, USA). Anti-CD44 and anti-CCR6 antibodies were supplied by Abcam (Cambridge, UK) and Novus Biologicals (USA), respectively. The In Situ Cell Death Detection Kit (50T) was obtained from Roche Diagnostics Ltd. (Switzerland). All other chemicals were obtained from Sinopharm Chemical Reagent Co., Ltd. (China).

Animals and cell lines

Male C57BL/6 mice (8–11 weeks old) were

provided by the Experimental Animal Center of Shanghai University of Traditional Chinese Medicine, and the protocol used was approved by the Experimental Animal Ethics Committee of Shanghai University of Traditional Chinese Medicine (License No. SYXK [HU] 2014-0008). The mice were housed in a specific pathogen-free (SPF), ventilated environment with regulated temperature (20 °C ± 5 °C) and humidity (50% ± 5%) and were fed *ad libitum*. These mice were used for experiments 1 week after adaptive feeding.

HaCaT cells were provided by the Cell Resource Center of the Institute of Basic Medical Sciences, Chinese Academy of Medical Sciences.

HPLC method for assaying curcumin

An HPLC instrument (LC-2010A HT, Shimadzu, Japan) with a C18 ODS column (5 μm, 250 × 4.6 mm; DIKMA, China) was used for the *in vitro* and *in vivo* detection of curcumin. The composition of the mobile phase was acetonitrile: 0.4% acetic acid (65:35, v/v) with a flow of 1 mL/min, and the column oven temperature was set at 30 °C. Samples were inspected at a detection wavelength of 428 nm. The limits of detection and quantitation were 0.1 and 0.5 μg/mL, respectively. The intra-day precision, inter-day precision, intra-day accuracy, and inter-day accuracy were 1.58%, 2.01%, 98.65%, and 99.20%, respectively. The studies were carried out at 25 °C in an air-conditioned laboratory.

Preparation of curcumin-loaded formulations

Synthesis of HA-conjugated DOPE

In total, 30.0 mg of HA, 1-(3-Dimethylamino-propyl)-3-ethylcarbodiimide hydrochloride (EDC) 57.6 mg, and 1-hydroxypyrrolidine-2,5-dione (NHS) 65.0 mg were dissolved in 10 mL of distilled water. The pH was adjusted to 7.5 with NaOH solution and reacted for 3 h at 37 °C in a water bath. A solution containing 72.0 mg of DOPE was added to the reaction solution, and the reaction was carried out in a water bath at 37 °C for 24 h. The reaction solution was dialyzed against 2,000 mL double distilled water and dialyzed every 10 h. Lyophilization yielded HA-conjugated DOPE (HA-DOPE), and it was identified by a Fourier transformation infrared spectrometer (FT-IR, R330; Thermo Fisher Scientific) (Fig. S1). The characteristic absorption peak of hydroxyl in HA was at 3419.92 cm^{-1}. The 2921.90 cm^{-1} and 1465.89 cm^{-1} absorption peaks indicated the characteristic long-chain methylene absorption peaks in DOPE, and 1379.34 cm^{-1} was the characteristic absorption peak of the carbonyl group in the ester bond of DOPE. In the infrared spectrum of HA-DOPE, the 3412.75 cm^{-1} and 1740.44 cm^{-1} absorption peaks indicated the hydroxyl and carbonyl groups in the ester bond of HA and DOPE, respectively, indicating that the HA-DOPE synthesis was successful.

HA-ES and ES formulation

The compositions of the HA-ES and ES are shown in Table 1. Briefly, curcumin, HSPC, DSPE-PEG2000, and cholesterol were dissolved in propylene glycol. The HA-DOPE PBS solution was slowly injected into the propylene glycol solution at 40 °C in a water bath with magnetic stirring at 300 rpm; it was then ultrasonicated (power, 300 W; time, 5 min) in an ice bath with a probe sonicator (JY92-IIN; Scientz, China). The curcumin propylene glycol solution (PGS) was prepared by dissolving the same amount of drug as HA-ES and ES in 25% propylene glycol aqueous solution.

Characteristics of the formulated preparations

The studies were carried out at 25 °C, and the relative humidity ranged from 45% to 65% in an air-conditioned laboratory.

Size distribution and zeta potential

The particle size distribution of the prepared HA-ES and ES was measured via dynamic light scattering (DLS) using the instrument Zetasizer Nano (Nanozs 90; Malvern Panalytical, UK), and the zeta potential was measured simultaneously. All the measurements were conducted at 25 °C, and each measurement was performed in triplicate.

Transmission electron microscopy

Sample was dropped onto the special copper mesh of the electron microscope; the excess liquid was removed with a filter paper; and 2% of phospho-tungstic acid solution was added for negative staining for 20 s. After natural drying, the samples were observed by transmission electron microscopy (TEM).

Entrapment efficiency

The entrapment efficiency (EE) of the tested formulations was determined by ultrafiltration with an ultrafiltration tube (molecular weight cut off: 50 kDa) and centrifugation at 3,000 ×*g* to completely filter out the dispersion medium. The filter cake was washed twice with 25% propylene glycol aqueous solution. The filtrate was combined, and the curcumin was analyzed by using HPLC. The EE was calculated according to equation 1.

$$EE\ (\%) = (Wt - Wf)/Wt \times 100 \quad \text{(Eq. 1)},$$

where Wt is the total amount of curcumin in the tested formulation and Wf is the curcumin dispersed outside the nanovesicles.

Table 1. Compositions of the curcumin-loaded hyaluronic acid (HA)-modified ethosomes (HA-ES), curcumin-loaded ES, and the compared curcumin 25% propylene glycol solution (PGS).

Formulations	Curcumin (%, w/v)	HSPC (%, w/v)	DSPE-PEG2000 (%, w/v)	Cholesterol (%, w/v)	Propylene glycol (%, v/v)	HA (%, w/v)
HA-ES	0.1	0.8	0.2	0.2	25	0.1
ES	0.1	0.8	0.2	0.2	25	/
PGS	0.1	/	/	/	25	/

In vitro release of curcumin

The tested formulation was poured into a dialysis bag (MWCO: 35 kDa), sealed, and immersed in 25% propylene glycol PBS solution. The medium was kept at 32 °C and mixed at 100 rpm with a magnetic stirrer. Samples were withdrawn at predetermined time intervals, while equal volumes of fresh medium preheated to 32 °C were added to maintain the sink condition. Samples were assayed using HPLC.

Stability of curcumin-loaded formulations

HA-ES and ES were stored at 4 °C. The size distribution, zeta potential, and EE were determined after being stored for 0, 7, and 15 days, to evaluate the formulation stability.

Curcumin permeation studies

In vitro topical and transdermal delivery

The hair on the backs of mice was shaved with an electric razor. The mice were then anesthetized and sacrificed. The back skin was excised and rinsed with normal saline, and the subcutaneous fat and fascia tissues were carefully removed and stored in the frozen state for future use.

Vertical diffusion cells were used for permeation studies. Normal saline containing 20% PEG 400 was used as the receiving liquid to meet the sink condition. The skin was fixed in the middle of the supply pool and the receiving pool, with the SC facing the supply pool. The tested formulations with a curcumin concentration of 1% (w/v) were placed in the supply pool, and the experiment was carried out at 32 °C ± 1 °C with magnetic stirring at 100 rpm. Samples were taken at the scheduled time point, and the same volume of fresh isothermal liquid was supplemented. After sampling, the skin surface was wiped with normal saline to remove residual tested formulations, cut into pieces, and homogenized with 10% DMSO by using a sonicator (360 W, 50 kHz) for 30 min. The extract was centrifuged at 4,000 ×*g* for 10 min, and the supernatant was obtained. Curcumin in the prepared samples was analyzed by HPLC.

In vivo skin retention

The hair from the backs of mice was carefully removed with an electric razor, and imiquimod ointment (IMQ) was applied at 25 mg/cm^2 once a day for 10 days to establish psoriasiform inflammation on the IMQ-treated skin region. Each mouse was fixed on a thermostat plate, and a cylindrical reservoir with a bottom area of 1 cm^2 was adhered to the inflamed skin of the back. Next, 0.3 mL of the tested formulation with a curcumin concentration of 0.1% (w/v) was administered. After 8 h, the animals were humanely sacrificed, and the regions of the skin that received the topical treatment were carefully cut off. Residual drug solution was washed off with normal saline, and the skin was cut into pieces, homogenized with 10% DMSO by using a sonicator, and centrifuged at 4,000 ×*g* for 10 min. The supernatant was detected by HPLC.

Confocal laser scanning microscopic imaging

The animals used, as well as the drug dosing protocol, were the same as the experimental protocol in section 2.7.2. The drug administration was sustained for 8 h, and thereafter, the skin was washed with normal saline. The skin region that received the effective topical and transdermal drug delivery was excised and cut into two parts. One part was cut into 0.5 × 0.5 cm^2 squares, and the skin thickness was optically scanned by using the z-axis of a confocal laser scanning microscope (CLSM, Carl Zeiss 710; Zeiss, Germany) with Ex/Em wavelength 425/515 nm. The micrographs obtained were recorded to analyze the corresponding depth travelled by nanovesicular formulations in 8 h. The other part was embedded with an optimal cutting temperature (OCT) compound, sliced with a freezing microtome (Leica CM 1950; Leica Biosystems Nussloch GmbH, Germany), and the fluorescence distribution was immediately observed by using CLSM with Ex/Em wavelength 425/515 nm.

Immunofluorescence of CD44 protein distribution in skin

The frozen section of mouse skin (3 μm) was allowed to stand at room temperature for 30 min, fixed in acetone at 4 °C for 10 min, washed with PBS, incubated with 3% H_2O_2 for 5 min, washed with PBS, and finally rinsed in PBS for 30 min. Samples were incubated with blocking solution (1% BSA-PBS) for 30 min, after which 1:100 diluted primary antibody was added. The samples were then placed in a wet box at 4

°C overnight. The primary antibody was discarded, and the samples were rinsed with PBS. Thereafter, 1:100 diluted FITC/TRITC-labeled secondary antibody (diluted with 1% BSA-PBS) was added to the samples, which were then incubated at 37 °C for 30 min. The secondary antibody was discarded, and the samples were then rinsed with PBS, followed by the addition of DAPI for 20 min to counterstain nuclei. The samples were then rinsed with PBS and mounted with 0.5 M Na_2CO_3–50% glycerol and finally observed under a fluorescence microscope (BX53; Olympus, Japan).

In vitro cell uptake

Cell culture

HaCaT cells were cultured in DMEM containing 10% fetal bovine serum and 1% penicillin–streptomycin at 37 °C in a 5% CO_2 incubator.

Detection of CD44 expression in cells by immunohistochemistry

Cells were cultured on a cover glass (Fisherbrand, Fisher Scientific, UK) and incubated with TNF-α at a final concentration of 100 ng/mL or an equal volume of normal saline as the control for 2 h. The medium was removed, and the cells were washed with PBS. Then, 4% paraformaldehyde was added, and the cells were fixed for 30 min, washed with PBS, incubated with 0.5% Triton X-100 for 20 min, washed with PBS again, incubated with 3% H_2O_2 for 15 min, washed with PBS, and then incubated with 5% BSA blocking buffer at 37 °C for 30 min. Excess fluid was removed, and the primary antibody was added. The samples were then stored at 4 °C for 24 h, returned to room temperature, and washed with PBS. The secondary antibody was then added at 37 °C for 30 min. DAB developer was added, followed by incubation for 5 min at room temperature. Mayer's hematoxylin counterstain was added, and the samples were then dehydrated and made transparent. The cover glass was sealed with gum and observed under the microscope.

Cell uptake

Cells were seeded at a density of 2 × 10^5 cells/well in a 6-well plate, cultured for 24 h, then cultured with or without TNF-α (final concentration, 100 ng/mL) for 2 h. Next, DMEM without FBS, containing the tested formulations with curcumin (final concentration, 4 μg/mL), was added, followed by incubation for 15 min or 30 min. After incubation, the cells were removed and washed with cold PBS, and 0.25% trypsin was added. The cells were collected by centrifugation, washed with cold PBS, and resuspended in 0.5 mL of PBS. The fluorescence intensity of the cells was measured by flow cytometry (FACS-Canto; Becton, Dickinson and Company, USA).

Intracellular co-localization of curcumin-loaded nanocarriers

Cells were seeded at a density of 1 × 10^5 cells/well in a 6-well plate. After 24 h of culture, TNF-α was added to cells to a final concentration of 100 ng/mL, cultured for 2 h, washed with PBS, treated with DMEM (no FBS) containing the tested formulations with curcumin at a final concentration of 4 μg/mL, and incubated at 37 °C for 30 min. Thereafter, the culture medium was removed, the cells were washed with cold PBS, and 50 nM LysoTracker Red prepared with DMEM without FBS was added. The cells were incubated at 37 °C for 30 min, and then Hoechst 33342 was added to a concentration of 10 μg/mL. The cells were incubated at 37 °C for 10 min; thereafter, the medium was removed, cells were washed with cold PBS, fixed with polyoxymethylene, and observed using CLSM (TCS SP8; Leica, Germany).

Effect of the tested formulations on HaCaT cell apoptosis

Cells were seeded in 6-well plates at 2 × 10^5 per well, cultured for 24 h, and were either not treated further or treated with TNF-α at a final concentration of 100 ng/mL. An equal volume of PBS was added to the control group. After incubation for 2 h, the tested formulations were treated with curcumin at a final concentration of 8.0 μg/mL, and incubation was continued for 46 h. Cells were incubated with 0.25% trypsin for 5 min, washed with serum-free medium, washed with PBS, and suspended with binding buffer. Annexin V was added to the cell suspension, incubated for 10 min, and centrifuged, and the supernatant was discarded. The cells were resuspended in binding buffer, stained with propidium iodide, and detected by flow cytometry.

Effect on imiquimod-induced psoriasiform inflammation in mice

Grouping and dosing methods

The mice were randomly divided into the following groups: normal control (Normal), model (Model), HA-ES without curcumin (HA-ES-empty), PGS, ES, HA-ES, and clobetasol propionate ointment (CP). Except for the Normal group, 25 mg/cm^2 IMQ was applied on the right ear once a day for 10 days. Except for the Normal and Model groups, 0.3 mL/cm^2 of the HA-ES-empty or curcumin preparation was applied on the right ear every day, and 45 mg/cm^2

was applied once daily for 10 days for the CP group [10].

Psoriasis area and severity index of the tested formulations

The clinical psoriasis area and severity index (PASI) was used to assess the inflammatory response in the auricles of mice [11]. The right ear skin was scored for erythema, scaling, and thickening of the outer ear (0 points, no obvious lesions; 1 point, slight; 2 points, moderate; 3 points, marked; 4 points, very marked). The sum of the scores obtained for erythema, scaling, and skin thickening (0–12) was used to evaluate the severity of inflammation. The score was taken once a day for 10 days from the date of administration.

Hematoxylin–eosin staining of ear skin tissue slices

The outer ear of mice was fixed in 4% paraformaldehyde for 24 h, dehydrated with ethanol, made transparent with xylene, embedded in paraffin, sliced, stained with hematoxylin–eosin (HE), sealed with neutral gum, and observed for histopathology under a microscope.

Cytokine mRNA transcription detection by quantitative real-time PCR

Trizol was added to the tissue samples (100–200 mg) and then homogenized. Thereafter, chloroform at 1/5 the volume of Trizol was added, and the samples were then emulsified and centrifuged at 12,000 ×*g* to separate the supernatant. The supernatant was added into an equal volume of isopropanol, mixed, and centrifuged. The supernatant was then discarded and the residue washed with 75% ethanol. The residue was dried at room temperature and dissolved in DEPC water. The total RNA was determined using a microplate reader (SpectraMax® 190; Molecular Devices, Silicon Valley, CA, USA) with an OD_{260}/OD_{280} = 1.91, and the extracted RNA was of high purity and free of protein and DNA residues.

Reverse transcription was performed with a PrimeScript™ RT reagent kit (for real-time PCR) (Takara Bio Inc., Japan) according to the manufacturer's instructions.

qRT-PCR was carried out with the SYBR® *Premix Ex Taq*™ II (Tli RNaseH Plus) (Takara Bio Inc.) on a LightCycler® 96 real-time PCR system (Roche, Switzerland), following the manufacturer's instructions. The primer sequences are listed in Table 2. The real-time PCR data were analyzed by the comparative CT method (2-ΔΔCt) [12].

Immunohistochemistry

After dewaxing and hydration, the paraffin sections were immediately immersed in 3% H_2O_2 methanol for 10 min and washed twice for 3 min each time. The protocol outlined in Section 2.8.2 was followed for immunohistochemical staining, and the analysis was performed.

Table 2. Primer sequences of mouse genes assayed by quantitative real-time PCR.

Primer	Base sequence	Tm (°C)	Transcription product (bp)
β-Actin-F	ACCCTAAGGCCAACCGTGAAA	62	193
β-Actin-R	ATGGCGTGAGGGAGAGCATA	61	
IL-17A-F	TCAGCGTGTCCAAACACTGAG	60.81	79
IL-17A-R	CGCCAAGGGAGTTAAAGACTT	58.22	
IL-17F-F	TGCTACTGTTGATGTTGGGAC	58.22	165
IL-17F-R	CAGAAATGCCCTGGTTTTGGT	59.31	
IL-22-F	ATGAGTTTTTCCCTTATGGGGAC	58.39	124
IL-22-R	GCTGGAAGTTGGACACCTCAA	60.48	
IL-1β-F	GAAATGCCACCTTTTGACAGTG	58.62	116
IL-1β-R	TGGATGCTCTCATCAGGACAG	59.24	
TNF-α-F	TCAAACCCTGGTATGAGCCC	59.38	154
TNF-α-R	ACCCATTCCCTTCACAGAGC	59.67	

Western blot analysis

Ear tissue was homogenized with lysate containing phenylmethanesulfonyl fluoride (1:100) with a homogenizer (Tissuelyser-24; Shanghai Jingxin Industrial Development Co., Ltd, China) at 60 Hz for 5 min. The protein concentration was determined by using BCA working solution at a wavelength of 562 nm. The sample solution was mixed with SDS-PAGE loading buffer at 4:1 and boiled for 10 min. Samples and protein markers (10–180 KD) were loaded separately. SDS-PAGE electrophoresis was performed using an electrophoresis apparatus (Bio-Rad Laboratories, Inc., Hercules, USA). The gel was removed and immersed in transfer buffer for 5 min. The transfer interlayer was assembled in the following order: foam pads, filter paper, gel, membrane, filter paper, and foam pads. The transfer clamp was placed in the transfer tank, and the buffer was added. The membrane transfer device (Tanon, Shanghai, China) was placed in ice water and transferred at 350 mA for 2 h. After the transfer was complete, the membrane was rinsed in double distilled water. The membrane was placed in a reaction box, followed by staining with 0.5 mL of Ponceau S. This was then immersed into milk buffer (prepared by TBST and nonfat dry milk) and rocked for 1 h. The primary antibody was added and incubated at 4 °C overnight. The film was washed with TBST, and a second antibody was added and rocked for 1 h; thereafter, it was washed with TBST and placed into a gel imaging instrument (ChemiQ4600; Clinx Science Instruments Co., Ltd., China). ECL luminescence reagent was added, and quantitative analysis was performed.

Data analysis

The mean ± standard deviation values were determined. The statistical differences between two samples were calculated by Student's *t*-test by using Excel 2007 software (Microsoft, USA), and differences were considered significant at $p < 0.05$.

Results and discussion

Characteristics of the prepared nanovesicles

HA is a water-soluble polymer, which can be encapsulated on the surface of liposomes via the formation of a gel with a network structure. However, when the concentration of liposomes changes greatly, HA molecules detach [13]. To enable the successful modification of HA on the surface of the ethosomes, HA and DOPE are covalently bonded. In the preparation of HA-ES, HA-DOPE can be inserted into the phospholipid bilayer, while the HA molecules are exposed on the surface of the vesicles. Medium-MW HA (240 kDa) was used in the preparation of HA-DOPE, because large-MW HA possesses strong intramolecular and intermolecular interactions, which may result in the easy detachment of HA-DOPE from the liposomal membrane. However, when the MW of HA is too small, the anchoring between HA and CD44 weakens, which may not result in the expected targeting effect [14-15]. In addition, HSPC and DSPE-PEG2000 were selected for forming phospholipid membranes, which can reduce oxidation and improve the stability of phospholipid vesicles. Ethanol is usually used for the preparation of ethosomes, but it is easily volatilized, irritating damaged skin; therefore, it is not suitable for psoriasis-induced skin inflammation [16]. Herein, the ethosomes were prepared using propylene glycol. Propylene glycol has very low toxicity and irritancy, with a high boiling point, low volatility at normal temperature, stable physicochemical properties, and good moisture retention [17]. It is widely used as a moisturizer in external preparations and cosmetics. An earlier study demonstrated propylene glycol-mediated liposomes to achieve greater *in vivo* skin deposition of a drug than by using traditional liposomes and ethanol-formed ethosomes, and the former are being used as skin delivery vehicles [18]. Propylene glycol has a lower viscosity and better solubility for curcumin than glycerol. During the preparation of ES, when the concentration of propylene glycol exceeded 30%, the viscosity of the system, as well as the particle size of the vesicles, markedly increased. When the propylene glycol concentration was less than 20%, the drug-loading of curcumin decreased. Therefore, the preferable concentration of propylene glycol was 25%. The HA-DOPE concentration in HA-ES should also be evaluated, because a very high HA density on the surface of the liposomal vesicles enhances the interaction between HA molecules, causing HA-DOPE to detach from the liposomal membrane, increasing the viscosity of the system. Notably, the insertion of excessive DOPE into the phospholipid bilayer may lead to drug leakage and a decrease in drug EE. We also found that excessive HA-DOPE in the ethosome solution resulted in a size distribution larger than 300 nm for the liposomal vesicles. Therefore, the final concentration in the preparation was selected as 1 mg/mL.

The formulated HA-ES formed a transparent emulsion, with the Tyndall phenomenon induced by laser, which is a characteristic of a colloidal solution (Fig. 1B). By TEM, both HA-ES and ES appeared to be spherical, and the particle size distribution was relatively uniform (Fig. 1C), which corresponded with the measured polydispersity index values of <0.3 (Fig. 1D). However, ES had a distinct shell-like structure, while the middle part of the HA-ES vesicle was very dark in color, with an unusually light colored surface. This may be due to the marked absorption of water by the HA molecules on the surface of the vesicles. Due to the high moisture retention of HA, the water entrapped in the HA gel network was not completely evaporated by drying.

After formulation within 24 h, the ES particle size measured by the DLS method increased a little after modification with HA (Fig. 2A), which is due to the swelling of hydrated HA molecules in the phospholipid vesicles. The carboxyl and hydroxyl groups contained in the HA molecule form intramolecular and intermolecular hydrogen bonds in an aqueous solution and also have a helical spatial conformation. This chemical structure makes it highly absorbent, and HA can retain about 1,000 times of its weight in water [19]. Each disaccharide unit in the HA molecule contains a carboxyl group, which dissociates into negative ions under physiological conditions and contributes to the negative charges on the surface of the HA-ES vesicle. Therefore, the zeta potential value of HA-ES was greater than that of ES ($p < 0.05$; Fig. 2B). Notably, the EE of HA-ES was significantly higher than that of ES ($p < 0.01$; Fig. 2C). Upon storage at 4 °C for 15 days, the size distribution, zeta potential value, and EE of HA-ES showed no statistical differences compared to the values observed upon storage for 0 day, while the particle size of ES increased, and the zeta potential and EE significantly decreased ($p < 0.01$). This indicates that the gel network formed by HA on the surface of the vesicles is effective in improving the stability of the formulation. Similar findings were reported by Ravar

et al. that HA-coated liposomes achieved greater stability than the uncoated formulations [20]. We also observed that drug EE declined upon storage at room temperature (about 25 °C) for 15 days (data not shown), which may be due to the intensified molecular motion of the phospholipids and cholesterol at high temperature, which enhanced the fluidity of the liposomal membrane, in addition to the easy detachment of HA-DOPE from the phospholipid vesicles, which is likely to cause drug leakage. These results suggested that HA-ES should be stored at a low temperature.

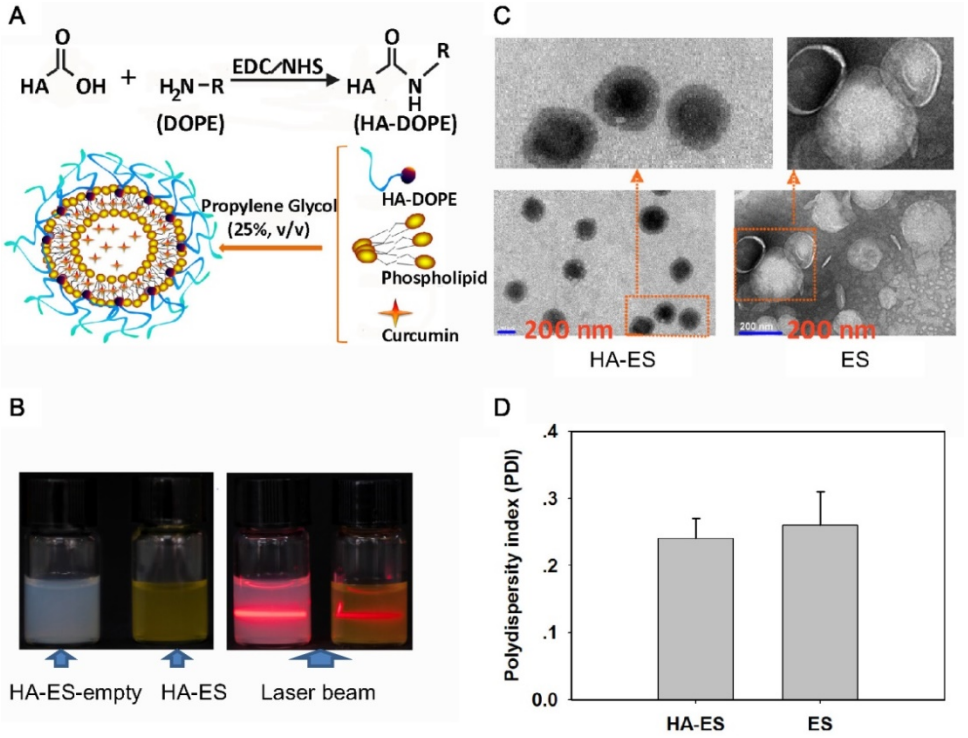

Figure 1. Characterization of HA-ES (A, diagram depicting vesicle formation; B, appearance and Tyndall characterization; C. TEM images; D. polydispersity index). HA, hyaluronic acid; HA-ES, curcumin-loaded HA-modified ethosomes; HA-ES-empty, HA-ES without curcumin; ES, curcumin-loaded ethosomes.

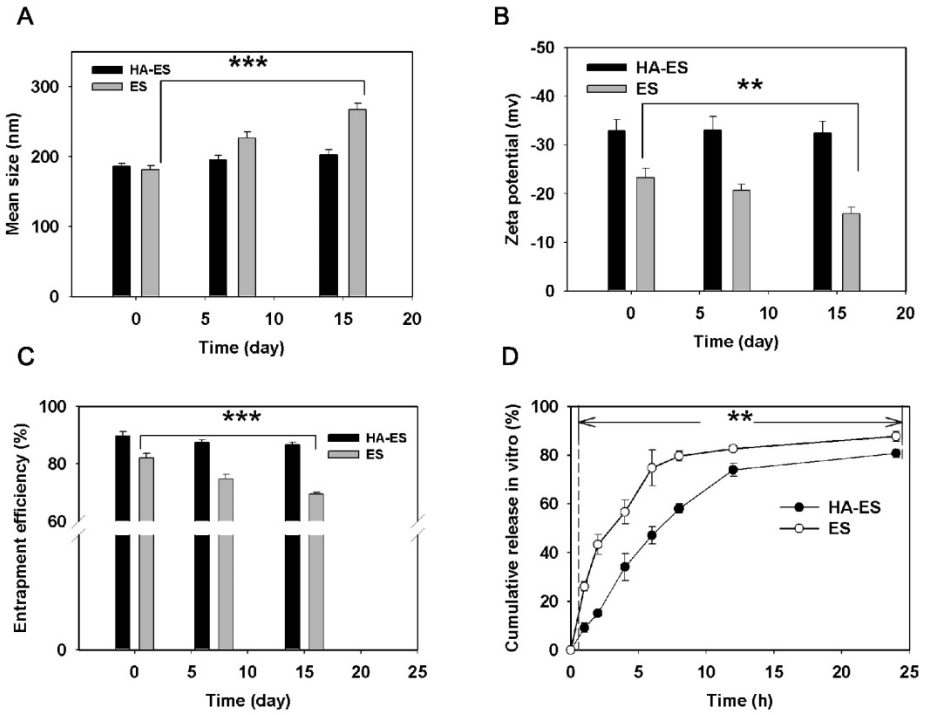

Figure 2. The stability (changes in: A, size distribution; B, zeta potential; C, entrapment efficiency; n = 3) at 4 °C and *in vitro* curcumin release (D; n = 3) of HA-ES and ES. **p < 0.01, ***p < 0.001. HA, hyaluronic acid; HA-ES, curcumin-loaded HA-modified ethosomes; ES, curcumin-loaded ethosomes.

HA immobilization resulted in a significantly lower *in vitro* release of curcumin from HA-ES than that of ES at each sampling time point ($p < 0.01$; Fig. 2D), and the drug release from ES in the first 1 h was 26%, while HA-ES showed a lower release of 9%. At 24 h, the cumulative release of curcumin from both ES and HA-ES exceeded 80%. The drug in HA-ES exhibited a sustained release behavior, indicating that the HA gel network hinders the diffusion of the fat-soluble curcumin molecules into the release medium via the phospholipid membrane and the HA gel layer. This could help the drug to be carried into the skin by HA-ES during topical administration, rather than the drug molecules being released followed by their entrapment outside the SC before the liposomal vesicles permeated into the skin [21].

Skin delivery of curcumin

As a promising topical delivery nanocarrier, two main approaches contribute to the high permeability of ethosomes: penetration and fusion mechanisms [22]. The penetration mechanism suggests that the low chain alcohol in the ethosomes enhances the flexibility and flow of the lipid bilayer membrane and acts as a penetration enhancer, which allows the ethosomes to fuse to the SC and penetrate the skin [23]. The fusion action based on the lipid-based ethosome membrane was similar to that of the SC; thus, they can fuse with each other, causing the disorganization of the hydrophobic group arrangement in the SC, and the consequent increase in fluidity and flexibility. This facilitates the entry of the ethosome-encapsulated drug into the intercellular spaces located deep in the skin via diffusion and capillary action to reach the dermis layer [24]. The ethosomes can also directly fuse with the cell membrane and release the drug into the cells via diffusion [25].

By encapsulating curcumin into ethosomes, topical and transdermal drug delivery was highly enhanced (Fig. 3). The current study showed that the cumulative transdermal amount of curcumin from HA-ES and ES was higher than that from PGS at each experimental time point. The PGS had a transdermal time lag of 0.5 h, while no similar disadvantage occurred for HA-ES and ES (Fig. 3A). After 8 h of topical administration, the cumulative transdermal amount and skin retention of curcumin in the HA-ES and the ES groups were, respectively, 3.32- and 2.30-fold higher than that in the PGS group, and the HA-ES group showed the highest drug permeability ($p < 0.05$; Fig. 3B); the cumulative drug amount in the receiving pool and in skin tissue reached 5.70 ± 0.81 μg/cm² and 15.17 ± 2.42 μg/cm², respectively. Moreover, as shown by CLSM, the HA-ES group

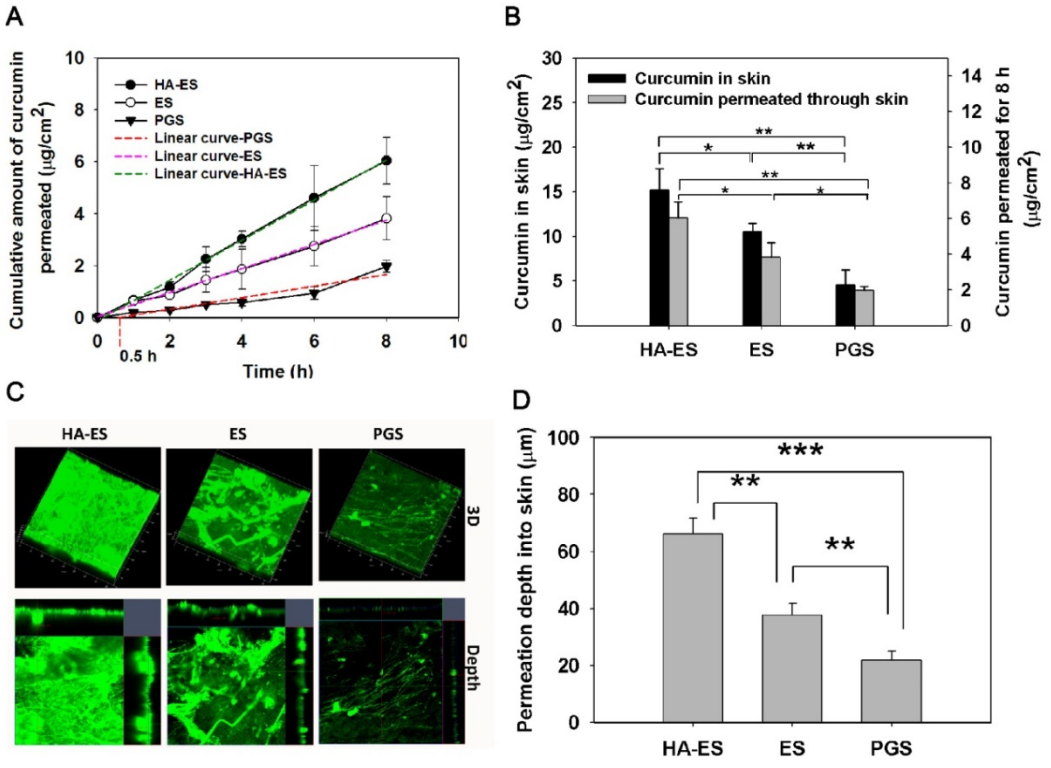

Figure 3. *In vitro* transdermal and dermal delivery of HA-ES, ES, and PGS in mouse skin after 8 h of topical administration (A, cumulative transdermal permeation; B, cumulative curcumin content in the skin (n = 3); C, CLSM tomography of psoriasis-like mouse skin; D, calculated curcumin permeation depth into the skin by CLSM tomography (n = 3). *p < 0.05, **p < 0.01, ***p < 0.001. HA, hyaluronic acid; HA-ES, curcumin-loaded HA-modified ethosomes; ES, curcumin-loaded ethosomes; PGS, curcumin 25% propylene glycol solution.

showed the strongest green autofluorescence in the skin indicative of curcumin (detectable fluorescence, 66.07 ± 5.58 μm) compared to the ES and PGS groups ($p < 0.01$). The curcumin fluorescence was the weakest in the skin of the PGS group, suggesting that the drug is less distributed in the skin (Fig. 3C–D) in contrast with the results for the other two ethosome groups. The results demonstrated the superiority of ES for topical curcumin delivery, and after HA modification, the percutaneous penetration of curcumin significantly increased compared with that for plain ES. Studies have found that there are cells that secrete inflammatory cytokines such as IL-17 and IL-22 in the dermis of the psoriatic skin lesions, and the delivery of curcumin to the deep skin layers helps to enhance the therapeutic effect by inhibiting the secretion of inflammatory cytokines [26].

As a matrix for external use, HA can increase the hydration of the SC through its excellent water absorption and moisturizing ability and increase the water content of the SC, thereby expanding and loosening the SC "brick wall" structure, improving the drug permeability, and increasing the accumulation of drugs in the skin [27]. Compared to non-polymeric micelle solutions containing similar amounts of drug, *in vitro* skin permeation analysis showed that the concentration of the drug in the epidermis and dermis increased by 3 and 6 times with the micelles formed by HA-synthesized polymers [28]. In Manca's report, HA-modified liposomes significantly increased the accumulation of curcumin in the epidermis and dermis compared to plain liposomes, suggesting that the HA gel network on the surface of phospholipid vesicles enhanced cutaneous drug absorption [29].

To further explore how HA-ES improves the absorption of curcumin in psoriatic skin, we used mouse models of IMQ-induced psoriasis-like inflammation for *in vivo* topical delivery experiments. After topical administration, the green autofluorescence of curcumin in skin slices from each treatment group was mainly distributed in the SC and epidermis, while the fluorescence was the strongest in the HA-ES group, with fluorescence observed clearly in the dermis and subcutaneous layers. The SC and epidermis of ES-treated skin showed less fluorescence distribution compared to the HA-ES group, with less fluorescence distribution below the epidermis. In the PGS group, only the SC and epidermis exhibited the weakest fluorescence distribution (Fig. 4A). Quantitative analysis of curcumin in the diseased skin by HPLC after *in vivo* administration showed that the skin drug retention in the HA-ES group was

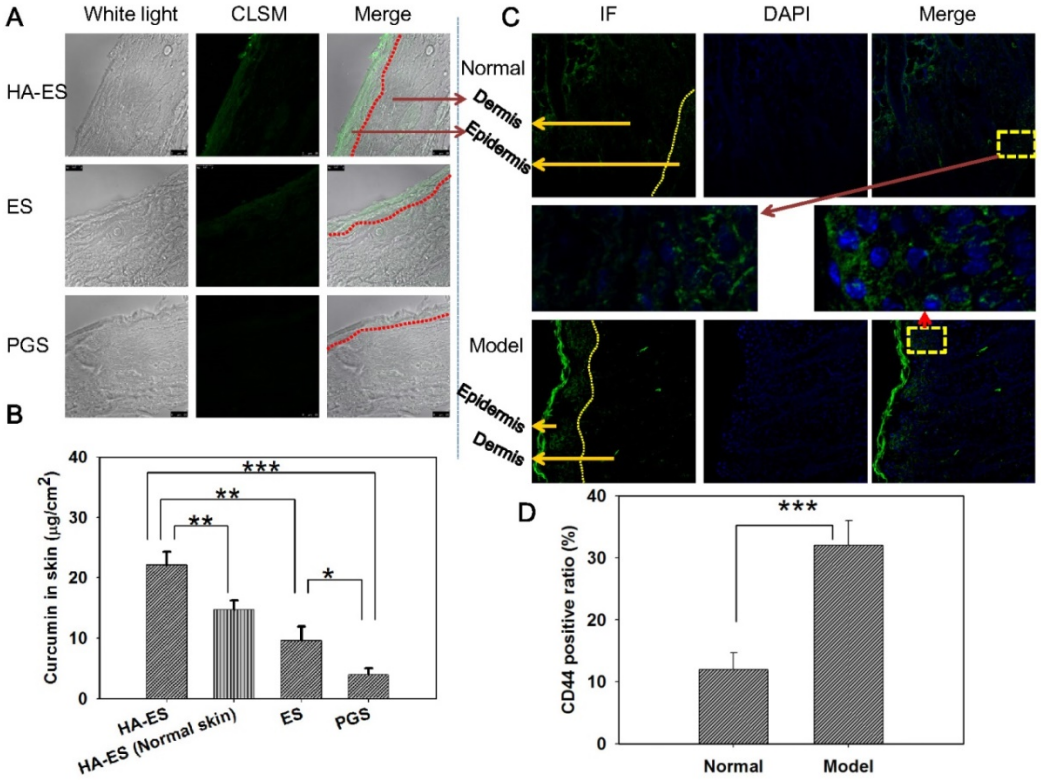

Figure 4. CLSM image (200× magnification) of curcumin fluorescence in frozen psoriasis-like mouse skin sections (A) and drug skin retention detected by HPLC (B; n = 5) after treatment with the various curcumin formulations for 8 h. The immunofluorescence images (C; 200× magnification) and semi-quantitative analysis (D; n = 5) show the distribution of CD44 expression in psoriasis-like and normal mouse skin. *p < 0.05, **p < 0.01, ***p < 0.001. Normal, mice treated without any formulations; Model, treated with IMQ only; HA, hyaluronic acid; HA-ES, curcumin-loaded HA-modified ethosomes; ES, curcumin-loaded ethosomes; PGS, curcumin 25% propylene glycol solution; IMQ, imiquimod ointment; IF, immunofluorescence.

significantly higher than that in the other three groups ($p < 0.01$), while the lowest amount of curcumin was assayed in the skin from the PGS group (Fig. 4B). These findings further confirm that HA-ES improves the topical absorption of drugs.

Next, we examined the distribution of CD44 protein in the skin of normal and psoriasis-like mice and found that staining for CD44, observed as green fluorescence, is mainly distributed in the epidermal layer in the normal skin. In the case of psoriasis-like skin, CD44 antibody fluorescence is mainly distributed in the epidermis, especially the stratum spinosum and basal cells of the thickened epidermis (Fig. 4C). The expression of CD44 protein in psoriasis-like skin was 2.7-fold higher than that in the normal skin ($p < 0.001$; Fig. 4D). These observations were in accordance with previous reports [8]. After the percutaneous administration of HA-ES, the accumulation of curcumin in psoriatic skin was significantly higher than that of normal skin (Fig. 4B). The fluorescence of curcumin from HA-ES was mainly distributed in the epidermal skin layer, where CD44 staining was highly expressed. This indicated that the nanovesicles permeated the skin after the application of HA-ES to psoriasis-like skin and could anchor to the surface of skin cells with high CD44 expression, which increased the accumulation of curcumin at the inflammation site and exerted drug effects for a sustained period.

In vitro cell uptake and apoptosis

Keratinocytes are the main cells of the human epidermis, which have a high proliferative and differentiation ability. The proliferation of keratinocytes can regulate epidermal cell growth and differentiation to form the SC and maintain the stability of the epidermis. Apoptosis of keratinocytes plays an important role in the induction of psoriasis [30]. As an inflammatory skin disease, psoriasis is characterized by excessive proliferation and abnormal differentiation and apoptosis of keratinocytes. *In vitro* culture of HaCaT cells is commonly used to screen anti-psoriatic drug candidates and evaluate the efficacy and mechanism of anti-psoriatic drugs [31]. After the co-incubation of HA-ES and ES with TNF-α-treated HaCaT cells, the green fluorescence of curcumin was mainly distributed in the cell membrane and was not observed in the nucleus (blue fluorescence, Fig. 5A), which was consistent with the intracellular distribution of free drug (PGS group). This indicates that after being encapsulated by the formulated phospholipid vesicles, the drug is mainly taken up by the cells via the phospholipid vesicles adhered to the cell membrane for lipid fusion, and the released drug molecules were internalized by diffusion (Fig. 5A) [32]. Compared with the PGS group, the curcumin-loaded nanovesicles did not change the intracellular drug distribution.

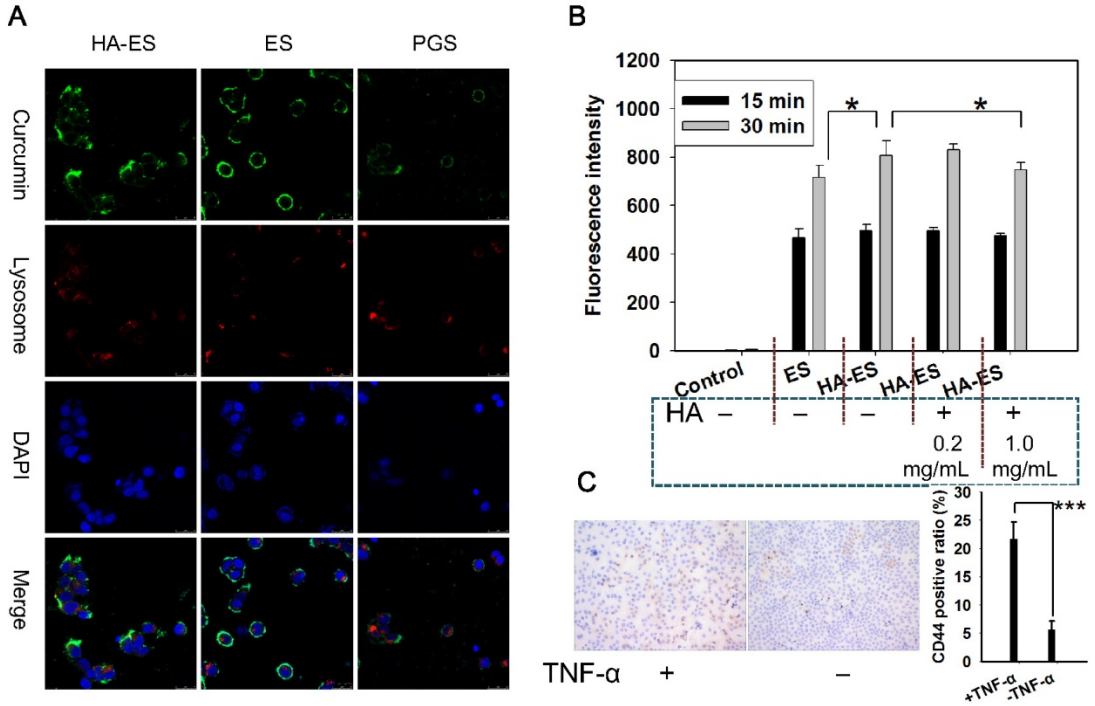

Figure 5. Uptake of curcumin by TNF-α-treated HaCaT cells (A, intracellular co-localization; B, curcumin fluorescence intensity in cells, n = 3) after incubation with curcumin formulations. Immunohistochemistry micrograph (C) showed marked CD44 expression in normal and TNF-α-treated HaCaT cells. *$p < 0.05$; ***$p < 0.001$. Control, normal cells treated without any formulations; HA, hyaluronic acid; HA-ES, curcumin-loaded HA-modified ethosomes; ES, curcumin-loaded ethosomes; PGS, curcumin 25% propylene glycol solution.

HaCaT cells showed a time-dependent relationship with the intake of curcumin in HA-ES and ES, and the intake at 30 min was significantly higher ($p < 0.05$) than that at 15 min. HaCaT cells that had been pre-incubated with 0.2 mg/mL or 1.0 mg/mL of HA in the medium showed no difference and significantly less uptake of curcumin from HA-ES, respectively, compared with cells that were not incubated with HA (Fig. 5B), indicating that HA at low concentration did not fully saturate CD44 on cell membranes. Immunohistochemical staining showed that CD44 expression in normal HaCaT cells was lower than that in TNF-α-treated HaCaT cells (Fig. 5C). HA-ES failed to adhere abundantly to HaCaT cells with overexpressed receptor proteins by incubation for too short a time (15 min), which might have led to no significant differences ($p > 0.05$) in the uptake of curcumin between the HA-ES and ES groups during the initial 15 min. An interesting observation was noted with respect to the cellular uptake of curcumin from the ES group, which showed a significant difference ($p < 0.05$) after being incubated for 30 min, mainly due to the HA-ES being specifically anchored to CD44 on the membranes of TNF-α-treated HaCaT cells. In addition, in association with the *in vitro* release study results, the release of the drug from ES in the culture medium was more than that from HA-ES; this could also be because of the free curcumin molecules being photodegraded or the difficulty in their uptake by cells owing to the poor water solubility and low apparent permeability coefficient [33-34].

Curcumin has been confirmed to inhibit the proliferation of HaCaT cells and induce apoptosis, which in turn improves the symptoms of psoriasis [35-36]. Compared to the control group, the apoptosis rates of HaCaT cells in different treatment groups increased, but no significant difference between the normal control group and TNF-α mono-treated control group ($p > 0.05$) were found. After nanocarrier entrapment, the apoptosis rate of curcumin in HaCaT cells was significantly higher than that of the free drug group (PGS), while the apoptosis rate of the HA-ES group was greater ($p < 0.05$) than that of the ES group, which was attributed to the enhanced cellular uptake of curcumin from HA-ES (Fig. 6A–B). We also found that upon treatment with HA-ES in the presence of TNF-α, the apoptosis rate of HaCaT cells was 3.1 times that of cells not induced by TNF-α (Fig. 6B), suggesting the stronger apoptosis of HaCaT cells than that of normal cells by curcumin. The current results also indicated that curcumin reversed the anti-apoptotic effect of TNF-α in HaCaT cells, highlighting its potential in psoriasis therapy [37-38].

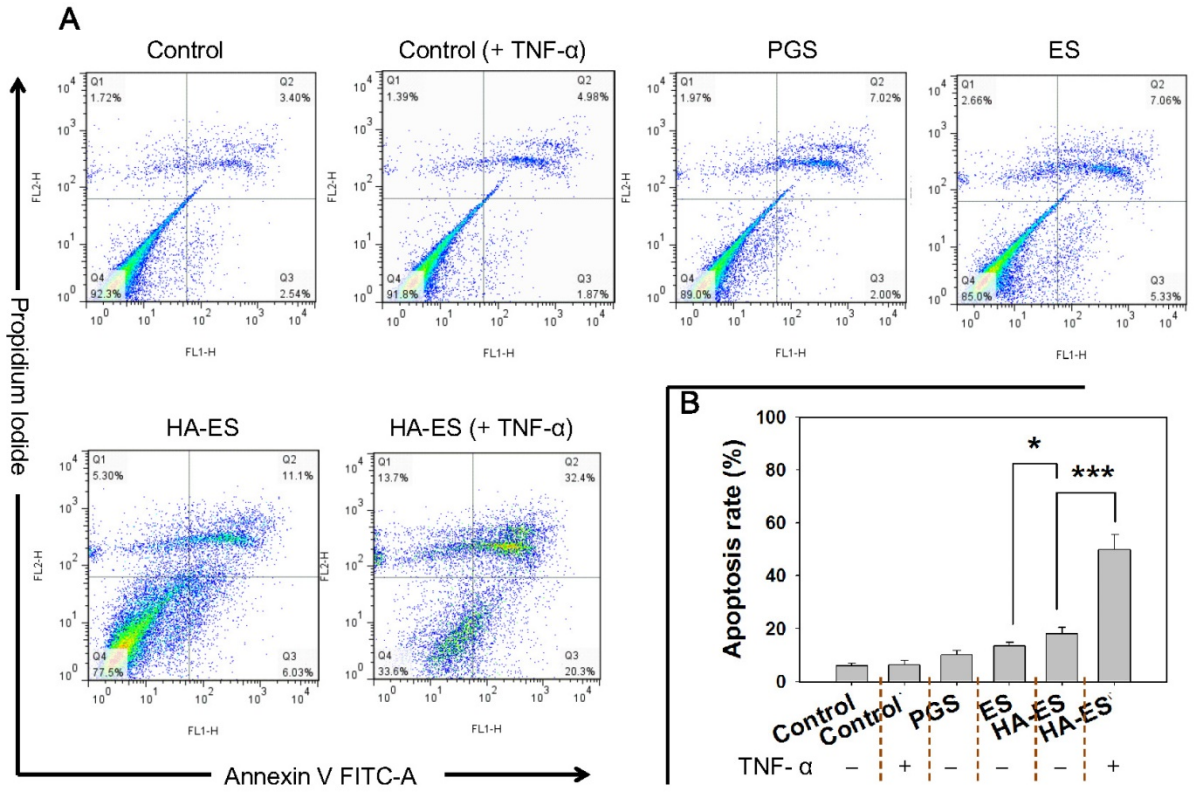

Figure 6. Apoptosis in HaCaT cells after incubation with curcumin formulations (A, flow cytometry apoptosis scatter plot; B, summed early and late apoptotic rate, n = 3). *p < 0.05, ***p < 0.001. Control, normal cells treated without any formulations; HA, hyaluronic acid; HA-ES, curcumin-loaded HA-modified ethosomes; ES, curcumin-loaded ethosomes; PGS, curcumin 25% propylene glycol solution.

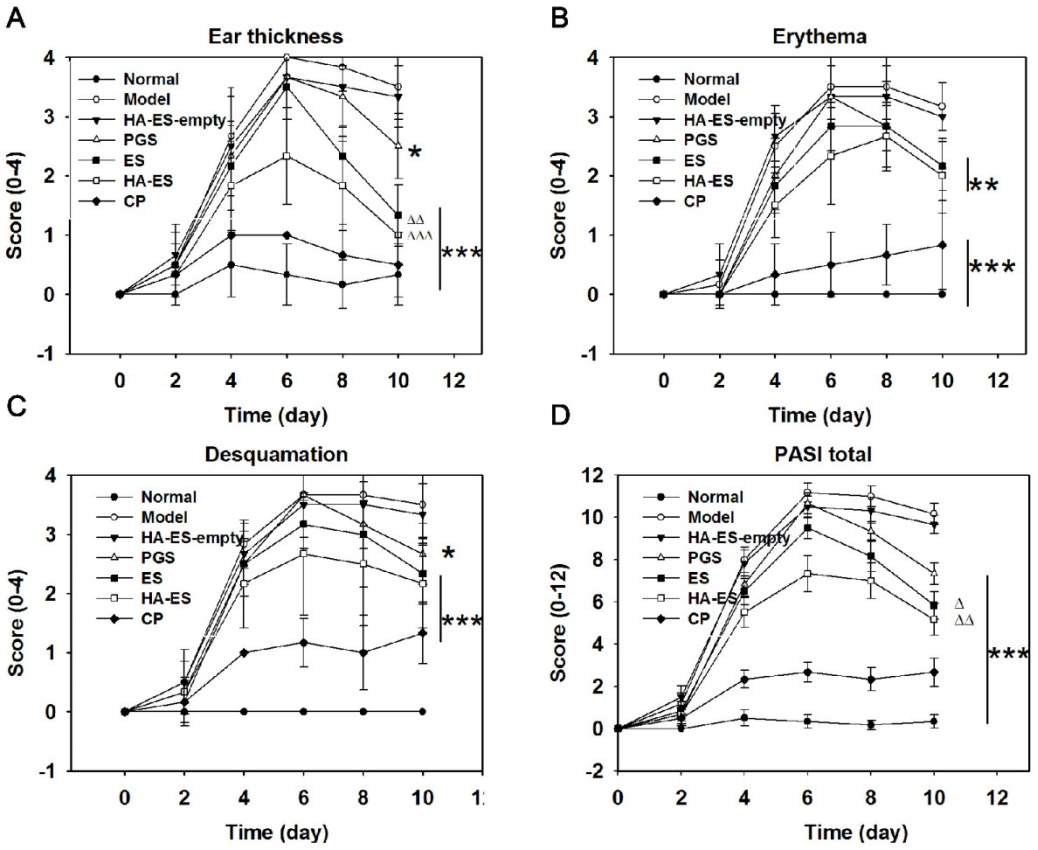

Figure 7. Psoriasis area and severity index (PASI) scores of IMQ-treated mouse ear, including ear thickness (A), erythema (B), desquamation (C), and total PASI (D), were evaluated after treatment with the various formulations (n = 6). Compared with model control, *p < 0.05, **p < 0.01, ***p < 0.001; HA-ES and ES compared with PGS, $^{\triangle}$p < 0.05, $^{\triangle\triangle}$p < 0.01. Normal, mice treated without any formulations; Model, treated with IMQ only; HA, hyaluronic acid; HA-ES, curcumin-loaded HA-modified ethosomes; HA-ES-empty, HA-ES without curcumin; ES, curcumin-loaded ethosomes; PGS, curcumin 25% propylene glycol solution; IMQ, imiquimod ointment; CP, clobetasol propionate cream.

In vivo antipsoriatic effect

Mice in the normal control group had normal feed intake and movement during the experiment. However, the IMQ-treated mice gradually developed mental fatigue and demonstrated body curling, decreased feed intake, and weight loss. IMQ caused skin irritation and decreased the glossiness of hair. After treatment with curcumin preparations and clobetasol propionate cream for alleviating symptoms, mice showed an improvement in their behavior and increase in feed intake. During the experiment, no abnormal secretion was found in the mouth, eyes, ears, or nose in any group. The stool and urine of the animals did not show any abnormalities either.

Compared with the normal control group, skin erythema was observed in the model group after 1 day of IMQ application; the skin appeared scaly in 2–3 days, with the most damage caused in 5–6 days, but the lesion slightly improved after 6 days, as shown in the day timepoints in Fig. 7. The auricle inflammatory response in mice was inhibited by the administration of curcumin preparations, but the effect was weaker than that of clobetasol propionate cream (Fig. 7). Correspondingly, the increase in ear thickness (Fig. S2), erythema, desquamation, and PASI scores of each IMQ-treated group were the highest on the 6th day, and the scores of the curcumin and clobetasol propionate groups showed a downward trend, indicating that the given drug had a therapeutic effect on the diseased skin. Notably, HA-ES had the strongest inhibitory effect on psoriatic skin symptoms within the tested curcumin preparations, and the PASI was only 0.77- and 0.69-fold than that of the ES and PGS groups (day 6 timepoint in Fig. 7), respectively. At the end of the experiment (day 10 timepoint in Fig. 7), the ear thickness, erythema, desquamation, and PASI scores of each group were significantly lower ($p < 0.05$) than those of the model group, and the vehicle (HA-ES-empty) showed no significant ($p > 0.05$) effect on the psoriasis-like symptoms (Fig. 7A–D); the ear thickness and PASI scores of the HA-ES and ES groups were, respectively, 0.40, 0.53 times, and 0.71, 0.80 times of those of the PGS group, while the PASI score of the HA-ES group was the lowest among the curcumin preparation groups.

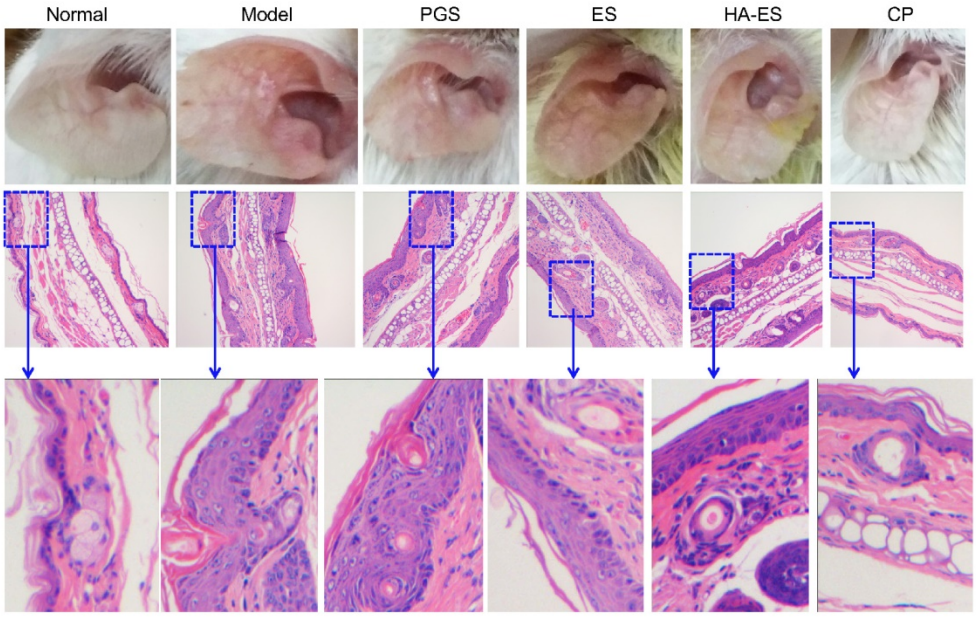

Figure 8. Appearance of the external auricle and micrographs (200× magnification) of hematoxylin and eosin-stained ear sections after the mice were treated with the various formulations for 10 days. Normal, mice treated without any formulations; Model, treated with IMQ only; HA, hyaluronic acid; HA-ES, curcumin-loaded HA-modified ethosomes; ES, curcumin-loaded ethosomes; PGS, curcumin 25% propylene glycol solution; IMQ, imiquimod ointment; CP, clobetasol propionate cream.

Fig. 8 shows the outer ear and HE staining of ear pathological slices of the mice in each experimental group at the end of the experiment. In the model control group, the auricle of the mice showed obvious psoriatic-like inflammatory reaction and skin thickening and erythema, and the skin lesions were severe. The inflammation of the auricle in the curcumin preparation-treated group was alleviated, especially ear erythema and desquamation, in the HA-ES group. The auricular inflammatory response of the clobetasol propionate group recovered markedly, and the ear appearance was similar to that of the normal control group.

A single layer of basal cells was observed inside the auricle of the normal group by HE staining of pathological slices (Fig. 8). The dermis layer was thin and reticular and had no papillary structure. Fat and blood vessels were distributed in the subcutaneous tissue, and muscle tissue was visible on the outside of the auricle. IMQ-induced skin thickening in the mouse auricle was caused by SC hyperplasia and subcutaneous tissue hyperplasia. In the model group, parakeratosis (residual nuclei) due to excessive proliferation of the SC cells and the "keratin pearl" formed by poor keratinization were observed, and the basal cells displayed a multi-layered arrangement. In addition, the normal linear structure of the dermis disappeared, irregular wrinkles appeared, and the reticular structure was blurred. The subcutaneous tissue cells increased, and a cluster-like proliferating cell population was observed. The curcumin preparations significantly inhibited the hyperplasia of the SC cells and subcutaneous tissue cells caused by IMQ. Among them, the recovery of the SC was the best in the HA-ES group. The SC of the clobetasol propionate-treated group was similar to that of the normal group.

Hyperproliferation of keratinocytes is associated with the induction of a variety of cytokines, such as TNF-α, IL-22, and IL-17, while causing keratinocytes to produce chemokines, cytokines, and antimicrobial peptides, thereby aggravating the inflammatory response. TNF-α is mainly produced by activated Th cells, monocytes, and macrophages, which promotes the secretion of IL-8 by keratinocytes, and it then recruits neutrophils to promote the proliferation of keratinocytes and induce psoriatic lesions [39]. IL-22 and IL-17 induce keratinocyte proliferation, leading to psoriatic lesions [40]. In addition, IL-17 synergizes with IFN-γ to induce the keratinocytes to secrete IL-6, IL-8, and other cytokines, and affect the normal proliferation and apoptosis of psoriatic keratinocytes [41]. In the process of psoriasis, IL-1β aggravates the condition by promoting the secretion of IL-17 by γδT cells [42-43].

The mRNA levels of TNF-α, IL-17A, IL-17F, IL-22, and IL-1β in the auricle skin of mice with psoriasis induced by IMQ were significantly higher than those of the normal control group ($p < 0.001$) (Fig. 9). However, each drug treatment significantly inhibited the expression of inflammatory factors ($p < 0.01$), especially clobetasol propionate treatment. The HA-ES and ES groups showed a stronger downregulation of the assayed cytokines than the PGS group, while the HA-ES treatment inhibited

IL-17A significantly more strongly than ES ($p < 0.001$).

IL-17A and IL-17F are mainly produced by γδT cells [44]. Curcumin and IMQ can stimulate the proliferation of epidermal γδT cells, and CCR6 is a marker for cells producing IL-17A [45-46]. In the present study, IMQ stimulated the expression of CCR6 in the mouse skin tissue (Fig. 10A), while curcumin and clobetasol propionate inhibited this upregulation ($p < 0.01$). The HA-ES and ES groups presented a stronger inhibitory effect on CCR6 expression than the PGS group ($p < 0.001$), and HA-ES treatment had a better effect on the downregulation of CCR6 than the ES treatment ($p < 0.01$) (Fig. 10B–C). Therefore, although the amount of γδT in the epidermis was increased by curcumin and IMQ, the expression of IL-17A and IL-17F was successfully inhibited by curcumin, an effect that was boosted by the developed HA-immobilized ethosomes.

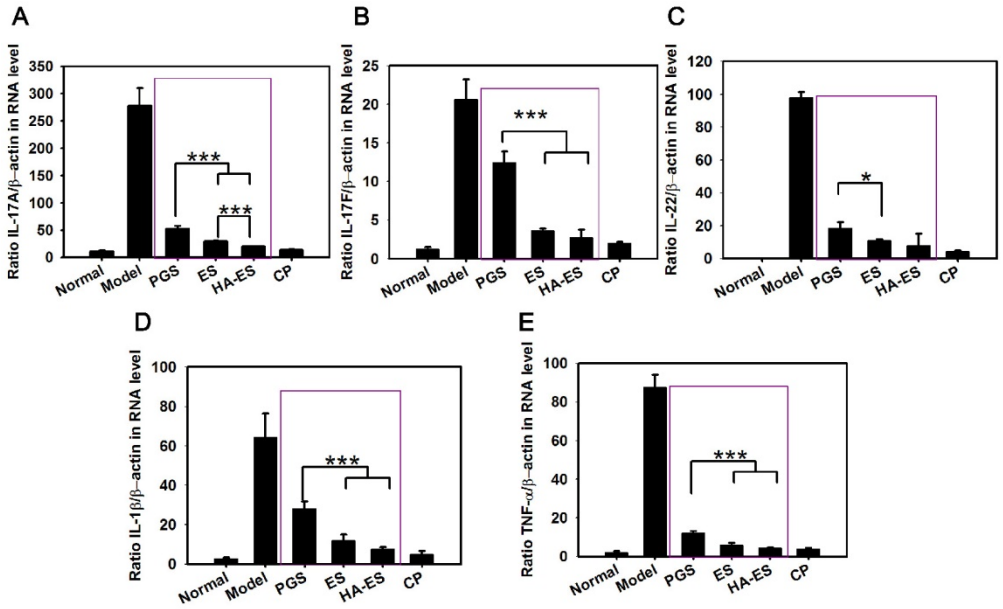

Figure 9. mRNA levels of IL-17A (A), IL-17F (B), IL-22 (C), IL-1β (D), and TNF-α (E) in the ear tissues of mice after treatment with the various formulations for 10 days, as measured by real-time PCR (n = 6). *p < 0.05, ***p < 0.001. Normal, mice treated without any formulations; Model, treated with IMQ only; HA, hyaluronic acid; HA-ES, curcumin-loaded HA-modified ethosomes; ES, curcumin-loaded ethosomes; PGS, curcumin 25% propylene glycol solution; IMQ, imiquimod ointment; CP, clobetasol propionate cream.

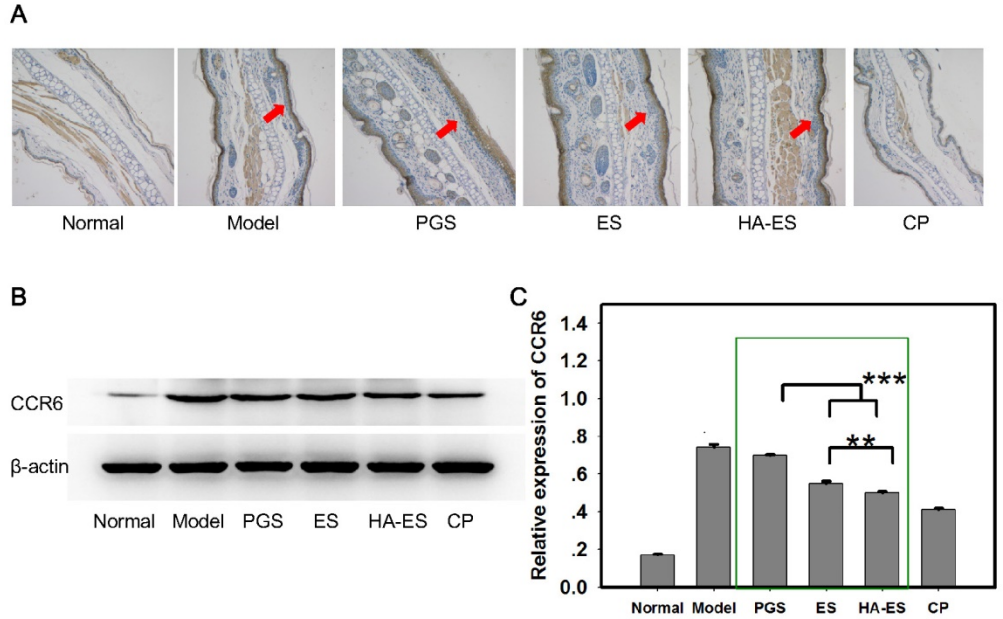

Figure 10. CCR6 protein expression in the ear tissues of mice after treatment with the various formulations (A, immunohistochemical micrograph, 200× magnification; arrows indicate CCR6 staining; B and C, western blot assay with β-actin as control, n = 6). **p < 0.01, ***p < 0.001. Normal, mice treated without any formulations; Model, treated with IMQ only; HA, hyaluronic acid; HA-ES, curcumin-loaded HA-modified ethosomes; ES, curcumin-loaded ethosomes; PGS, curcumin 25% propylene glycol solution; IMQ, imiquimod ointment; CP, clobetasol propionate cream.

Conclusion

We successfully developed HA-modified ethosomes with propylene glycol as a novel drug carrier for curcumin. The gel network formed by HA on the surface of phospholipid vesicles effectively reduced drug leakage, improved the stability of the preparation, and allowed the slow release of the loaded curcumin. The HA-ES system targeted the CD44 protein, which is overexpressed in inflamed psoriatic skin, to achieve targeted delivery of drugs, thereby increasing the accumulation of curcumin in inflamed skin. Topical administration of HA-ES improved the therapeutic effect on imiquimod-induced psoriatic-like inflamed skin of mice. In summary, by targeting the highly expressed CD44 protein in the inflamed skin, this promising topical delivery system may also be used to increase the accumulation of other anti-psoriatic drugs.

Supplementary Material

Supplementary figures and tables.
http://www.thno.org/v09p0048s1.pdf

Acknowledgements

This work was financially supported by the National Natural Science Foundation of China (81673612, 81573619).

Competing Interests

The authors have declared that no competing interest exists.

References

1. Boehncke WH, Schön MP. Psoriasis. Lancet. 2015; 386: 983-94.
2. Rahman M, Akhter S, Ahmad J, Ahmad MZ, Beg S, Ahmad FJ. Nanomedicine-based drug targeting for psoriasis: potentials and emerging trends in nanoscale pharmacotherapy. Expert Opin Drug Deliv. 2015;12:635-52.
3. Doppalapudi S, Jain A, Chopra DK, Khan W. Psoralen loaded liposomal nanocarriers for improved skin penetration and efficacy of topical PUVA in psoriasis. Eur J Pharm Sci. 2017;96:515-29.
4. Cevc G, Blume G. Hydrocortisone and dexamethasone in very deformable drug carriers have increased biological potency, prolonged effect, and reduced therapeutic dosage. Biochim Biophys Acta. 2004;1663:61-73.
5. Touitou E, Dayan N, Bergelson L, Godin B, Eliaz M. Ethosomes - novel vesicular carriers for enhanced delivery: characterization and skin penetration properties. J Control Release. 2000;65: 403-18.
6. Dubey V, Mishra D, Dutta T, Nahar M, Saraf DK, Jain NK. Dermal and transdermal delivery of an anti-psoriatic agent via ethanolic liposomes. J Control Release. 2007;123:148-54.
7. Zhang YT, Shen LN, Wu ZH, Zhao JH, Feng NP. Comparison of ethosomes and liposomes for skin delivery of psoralen for psoriasis therapy. Int J Pharm. 2014;471:449-52.
8. Lindqvist U, Phil-Lundin I, Engström-Laurent A. Dermal Distribution of hyaluronan in psoriatic arthritis; coexistence of CD44, MMP3 and MMP9. Acta Derm Venereol. 2012; 92: 372-7.
9. Lv Y, Xu C, Zhao X, Lin C, Yang X, Xin X, et al. Nanoplatform Assembled from a CD44-Targeted Prodrug and Smart Liposomes for Dual Targeting of Tumor Microenvironment and Cancer Cells. ACS Nano. 2018;12:1519-36.
10. Pischon H, Radbruch M, Ostrowski A, Schumacher F, Hönzke S, Kleuser B, et al. How Effective Is Tacrolimus in the Imiquimod-Induced Mouse Model of Psoriasis? J Invest Dermatol. 2018;138:455-8.
11. van der Fits L, Mourits S, Voerman JS, Kant M, Boon L, Laman JD, et al. Imiquimod-induced psoriasis-like skin inflammation in mice is mediated via the IL-23/IL-17 axis. J Immunol. 2009; 182: 5836-45.
12. Schmittgen TD, Livak KJ. Analyzing real-time PCR data by the comparative C(T) method. Nat Protoc. 2008; 3: 1101-8.
13. Taetz S, Bochot A, Surace C, Arpicco S, Renoir JM, Schaefer UF, et al. Hyaluronic acid-modified DOTAP/DOPE liposomes for the targeted delivery of anti-telomerase siRNA to CD44-expressing lung cancer cells. Oligonucleotides. 2009; 19: 103-16.
14. Zhao N, Wang X, Qin L, Guo Z, Li D. Effect of molecular weight and concentration of hyaluronan on cell proliferation and osteogenic differentiation in vitro. Biochem Biophys Res Commun. 2015; 465: 569-74.
15. Qhattal HS, Hye T, Alali A, Liu X. Hyaluronan polymer length, grafting density, and surface poly(ethylene glycol) coating influence in vivo circulation and tumor targeting of hyaluronan-grafted liposomes. ACS Nano. 2014; 8: 5423-40.
16. Farkas A, Kemény L. Alcohol, liver, systemic inflammation and skin: a focus on patients with psoriasis. Skin Pharmacol Physiol. 2013; 26: 119-26.
17. Fiume MM, Bergfeld WF, Belsito DV, Hill RA, Klaassen CD, Liebler D, et al. Safety assessment of propylene glycol, tripropylene glycol, and PPGs as used in cosmetics. Int J Toxicol. 2012; 31: 245S-60S.
18. Elsayed MM, Abdallah OY, Naggar VF, Khalafallah NM. PG-liposomes: novel lipid vesicles for skin delivery of drugs. J Pharm Pharmacol. 2007;59:1447-50.
19. Stern R, Asari AA, Sugahara KN. Hyaluronan fragments: an information-rich system. Eur J Cell Biol. 2006; 85: 699-715.
20. Ravar F, Saadat E, Gholami M, Dehghankelishadi P, Mahdavi M, Azami S, et al. Hyaluronic acid-coated liposomes for targeted delivery of paclitaxel, in-vitro characterization and in-vivo evaluation. J Control Release. 2016; 229: 10-22.
21. Carita AC, Eloy JO, Chorilli M, Lee RJ, Leonardi GR. Recent Advances and Perspectives in Liposomes for Cutaneous Drug Delivery. Curr Med Chem. 2018; 25: 606-35.
22. Dubey V, Mishra D, Jain NK. Melatonin loaded ethanolic liposomes: physicochemical characterization and enhanced transdermal delivery. Eur J Pharm Biopharm. 2007; 67: 398-405.
23. Tosato MG, Maya Girón JV, Martin AA, Krishna Tippavajhala V, Fernández Lorenzo de Mele M, Dicelio L. Comparative study of transdermal drug delivery systems of resveratrol: High efficiency of deformable liposomes. Mater Sci Eng C Mater Biol Appl. 2018; 90: 356-64.
24. Das SK, Chakraborty S, Roy C, Rajabalaya R, Mohaimin AW, Khanam J, et al. Ethosomes as Novel Vesicular Carrier: An Overview of the Principle, Preparation and its Applications. Curr Drug Deliv. 2018; 15: 795-817.
25. Yang L, Wu L, Wu D, Shi D, Wang T, Zhu X. Mechanism of transdermal permeation promotion of lipophilic drugs by ethosomes. Int J Nanomedicine. 2017; 12: 3357-64.
26. Lowes MA, Kikuchi T, Fuentes-Duculan J, Cardinale I, Zaba LC, Haider AS, et al. Psoriasis vulgaris lesions contain discrete populations of Th1 and Th17 T cells. J Invest Dermatol. 2008;128:1207-11.
27. Law CH, Li JM, Chou HC, Chen YH, Chan HL.Hyaluronic acid-dependent protection in H9C2 cardiomyocytes: a cell model of heart ischemia-reperfusion injury and treatment. Toxicology. 2013; 303: 54-71.
28. Šmejkalová D, Muthný T, Nešporová K, Hermannová M, Achbergerová E, Huerta-Angeles G, et al. Hyaluronan polymeric micelles for topical drug delivery. Carbohydr Polym. 2017; 156: 86-96.
29. Manca ML, Castangia I, Zaru M, Nácher A, Valenti D, Fernàndez-Busquets X, et al. Development of curcumin loaded sodium hyaluronate immobilized vesicles (hyalurosomes) and their potential on skin inflammation and wound restoring. Biomaterials. 2015; 71: 100-9.
30. Wang M, Zhang S, Zheng G, Huang J, Songyang Z, Zhao X, et al. Gain-of-Function Mutation of Card14 Leads to Spontaneous Psoriasis-like Skin Inflammation through Enhanced Keratinocyte Response to IL-17A. Immunity. 2018; 49: 66-79.e5.
31. Nikolova B, Kostadinova A, Dimitrov B, Zhelev Z, Bakalova R, Aoki I, et al. Fluorescent imaging for assessment of the effect of combined application of electroporation and rifampicin on HaCaT cells as a new therapeutic approach for psoriasis. Sensors (Basel). 2013; 13: 3625-34.
32. Jiang X, Xin H, Ren Q, Gu J, Zhu L, Du F, et al. Nanoparticles of 2-deoxy-D-glucose functionalized poly(ethylene glycol)-co-poly(trimethylene carbonate) for dual-targeted drug delivery in glioma treatment. Biomaterials. 2014; 35: 518-29.
33. Ahmad MZ, Akhter S, Mohsin N, Abdel-Wahab BA, Ahmad J, Warsi MH, et al. Transformation of curcumin from food additive to multifunctional medicine: nanotechnology bridging the gap. Curr Drug Discov Technol. 2014;11:197-213.
34. Nelson KM, Dahlin JL, Bisson J, Graham J, Pauli GF, Walters MA. The Essential Medicinal Chemistry of Curcumin. J Med Chem. 2017; 60: 1620-37.
35. Varma SR, Sivaprakasam TO, Mishra A, Prabhu S, M R, P R. Imiquimod-induced psoriasis-like inflammation in differentiated Human keratinocytes: Its evaluation using curcumin. Eur J Pharmacol. 2017; 813: 33-41.
36. Sun L, Liu Z, Wang L, Cun D, Tong HHY, Yan R, et al. Enhanced topical penetration, system exposure and anti-psoriasis activity of two particle-sized, curcumin-loaded PLGA nanoparticles in hydrogel. J Control Release. 2017; 254: 44-54.
37. Lundvig DM, Pennings SW, Brouwer KM, Mtaya-Mlangwa M, Mugonzibwa E, Kuijpers-Jagtman AM, et al. Cytoprotective responses in HaCaT keratinocytes exposed to high doses of curcumin. Exp Cell Res. 2015; 336: 298-307.

38. Sun J, Han J, Zhao Y, Zhu Q, Hu J. Curcumin induces apoptosis in tumor necrosis factor-alpha-treated HaCaT cells. Int Immunopharmacol. 2012;13:170-4.
39. Rahman M, Alam K, Ahmad MZ, Gupta G, Afzal M, Akhter S, et al. Classical to current approach for treatment of psoriasis: a review. Endocr Metab Immune Disord Drug Targets. 2012;12:287-302.
40. Takahashi T, Koga Y, Kainoh M. Anti-IL-12/IL-23p40 antibody ameliorates dermatitis and skin barrier dysfunction in mice with imiquimod-induced psoriasis-like dermatitis. Eur J Pharmacol. 2018; 828: 26-30.
41. Nograles KE, Zaba LC, Guttman-Yassky E, Fuentes-Duculan J, Suárez-Fariñas M, Cardinale I, et al. Th17 cytokines interleukin (IL)-17 and IL-22 modulate distinct inflammatory and keratinocyte-response pathways. Br J Dermatol. 2008; 159: 1092-102.
42. Coffelt SB, Kersten K, Doornebal CW, Weiden J, Vrijland K, Hau CS, et al. IL-17-producing γδ T cells and neutrophils conspire to promote breast cancer metastasis. Nature. 2015; 522: 345-8.
43. Sutton CE, Lalor SJ, Sweeney CM, Brereton CF, Lavelle EC, Mills KH. Interleukin-1 and IL-23 induce innate IL-17 production from gammadelta T cells, amplifying Th17 responses and autoimmunity. Immunity. 2009; 31: 331-41.
44. Roark CL, Simonian PL, Fontenot AP, Born WK, O'Brien RL. gammadelta T cells: an important source of IL-17. Curr Opin Immunol. 2008; 20: 353-7.
45. Kagami S, Rizzo HL, Lee JJ, Koguchi Y, Blauvelt A. Circulating Th17, Th22, and Th1 cells are increased in psoriasis. J Invest Dermatol. 2010; 130: 1373-83.
46. Cai Y, Shen X, Ding C, Qi C, Li K, Li X, et al. Pivotal role of dermal IL-17-producing γδ T cells in skin inflammation. Immunity. 2011; 35: 596-610.